NASA TECHNICAL NOTE

NASA TN D-2299

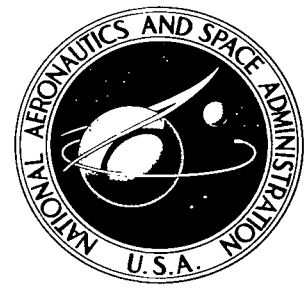

NASA TN D-2299

FORCES ACTING ON BUBBLES IN NUCLEATE BOILING UNDER NORMAL AND REDUCED GRAVITY CONDITIONS

by Edward G. Keshock and Robert Siegel

Lewis Research Center
Cleveland, Ohio

NATIONAL AERONAUTICS AND SPACE ADMINISTRATION • WASHINGTON, D. C. • AUGUST 1964

ERRATA

NASA TECHNICAL NOTE D-2299

Completed 12 Jan 65 Lila

FORCES ACTING ON BUBBLES IN NUCLEATE BOILING UNDER NORMAL AND REDUCED GRAVITY CONDITIONS

by Edward G. Keshock and Robert Siegel

August 1964

Page 21: The last line should read

was significant, an approximate drag force was computed from equation (6). For

NASA-Langley, 1964

Issued 12-18-64

FORCES ACTING ON BUBBLES IN NUCLEATE BOILING UNDER NORMAL AND REDUCED GRAVITY CONDITIONS

By Edward G. Keshock and Robert Siegel

Lewis Research Center
Cleveland, Ohio

NATIONAL AERONAUTICS AND SPACE ADMINISTRATION

For sale by the Office of Technical Services, Department of Commerce,
Washington, D.C. 20230 -- Price $0.75

FORCES ACTING ON BUBBLES IN NUCLEATE BOILING UNDER NORMAL AND REDUCED GRAVITY CONDITIONS

by Edward G. Keshock and Robert Siegel

Lewis Research Center

SUMMARY

An experimental study was made of bubble growth, departure, and rise during nucleate boiling in saturated aqueous-sucrose solutions, ranging from 20- to 60-percent sucrose by weight, in seven different gravity fields from 1.4 to 100 percent of Earth gravity. Results are compared with similar data from a previous study of nucleate boiling in saturated distilled water. In the present study, the departure diameters unexpectedly exhibited no gravity dependence in contrast to the data for saturated water where departure diameters varied approximately as $g^{-1/2}$. The difference in behavior was explained by calculating, from the experimental data throughout a bubble growth period, various forces believed to influence the bubble departure. Departure was found to be dependent on the relative magnitudes of the buoyancy, inertial, and surface-tension forces, with the viscous drag being of little significance. The bubbles in sucrose solutions proved to be inertia dominated, and hence gravity independent, while the departure of the bubbles in water was governed by buoyancy, and hence gravity dependent. The rise of bubbles through the liquid after departure was analyzed, and the predicted rise rates agreed reasonably well with those observed.

INTRODUCTION

The advent of space travel has stimulated interest in the effects of gravity on various fluid mechanical and heat-transfer processes. One process that would be expected to be gravity dependent is nucleate pool boiling in a saturated liquid, since the gravitational buoyancy force contributes to the detachment of vapor bubbles from the surface and then causes them to rise through the liquid.

Some recent experiments in reduced gravity fields (refs. 1 to 3) have measured the heat flux and the temperature difference between a heated surface and liquid in the nucleate boiling range and have investigated the dependence of the critical (burnout) heat flux on gravity. These experiments were limited by the short durations of the low-gravity period available, but they did indicate

some significant characteristics. In the nucleate boiling range, the curve of heat flux as a function of temperature difference was found to be essentially independent of gravity. The curve was shifted within only a degree of temperature difference when gravity was varied in the range between Earth gravity and zero. The burnout heat flux varied approximately as gravity to the one quarter power as indicated by theory.

In order to obtain a more fundamental understanding of how reduced gravity influences the nucleate boiling process, a study of bubble dynamics in partial gravity fields was initiated using a counterweighted drop-tower facility (ref. 4). Boiling took place from a polished horizontal surface at low heat fluxes so that only a few nucleation sites were active and individual bubbles could be photographed. In low-gravity fields, the nucleation of a single column of bubbles exhibited a cyclical behavior as follows: A fully grown bubble would detach and remain close to the surface because of the low rise velocity in reduced gravity. A number of bubbles issuing from the same nucleation site are then absorbed by the detached bubble during the early stages of their growth. As the vapor mass formed by the coalescence of these bubbles moves slowly upward, it eventually rises sufficiently far above the surface that the next bubble formed does not join with it and the cycle is then repeated. Hence, in low-gravity nucleate boiling, the vapor mass, which tends to remain near the surface, serves as a means for removing subsequent bubbles from the surface while they are still very small. This bubble removal would tend to increase the bubble frequency and turbulence near the surface and thereby maintain a high heat-transfer coefficient. The tendency of vapor to linger near the surface, however, probably accounts for the lowering of the critical (burnout) heat flux.

The reduction of buoyant forces in reduced gravity has directed increased attention to the other forces, such as surface tension and inertial, that might assume greater significance. This reduction has been discussed in references 3, 5, and 6, where the inertial and buoyancy forces were evaluated by utilizing a theoretical expression for the bubble growth rate such as given in reference 7. In reference 3, the Froude number, which is the ratio of inertial to buoyancy force, was computed for a single bubble under normal gravity conditions and found to vary from 452 for liquid nitrogen to 14,000 for water for representative values of bubble size and surface superheat. This would imply that the inertial force would be strongly dominating in the bubble dynamics. In reference 6, however, a similar discussion of the Froude number, which used the data of reference 1, indicated that for bubbles in water under both normal and reduced gravity conditions the inertia and buoyancy were of the same order of magnitude. Chun (ref. 8) obtained measurements of bubbles and computed buoyancy and surface-tension forces for boiling saturated water under normal gravity conditions. His results indicated a net upward force acting on the bubbles during growth. Hence, bubble departure was not believed to be governed by an equilibrium of these forces. The inertial force was not considered.

The purpose of the present work was to obtain detailed photographs of individual bubbles in nucleate boiling for reduced gravity conditions, and to compute from the bubble dimensions throughout the growth period the magnitudes of the forces that might significantly influence bubble departure. This approach is in contrast with the previously mentioned theoretical discussions in which

the forces were computed from growth relations that represent physical behavior only in an average way and hence may obscure some features. For example, in references 4 and 9, it is experimentally determined that the bubble growth in the early stages could be much more rapid than that predicted by existing theories. This higher growth rate could produce a high inertial force that might tear the bubble away from the surface before it grew very large. In this situation, the buoyancy forces would not be important, and the detachment of bubbles would be insensitive to gravity. Conversely, for a slowly growing bubble, the inertial forces will be small, and the bubble detachment will depend on an equilibrium between buoyancy and surface-tension forces. This will be a gravity dependent situation. Experimental results for both of these types of bubbles will be presented, and the forces acting on them discussed and interpreted in relation to the observed effects of gravity on bubble departure.

After detachment, the removal of the vapor from the vicinity of the surface depends on the buoyancy and drag forces. Some data on the bubble rise after detachment will be presented for several reduced gravity fields and compared with theory.

A motion-picture film showing boiling in normal and in reduced gravity of water, 60-percent aqueous-sucrose solution, and ethyl alcohol has been prepared and is available on loan. A request card and a description of the film are given at the back of this report.

SYMBOLS

C_d drag coefficient

D bubble diameter

D_b contact circle diameter (width of bubble base)

Eö Eötvös number

F force

g gravitational field

m apparent mass of bubble

P_b pressure outside bubble at its base

p_b pressure inside bubble at its base

q heat transferred per unit area and time from solid surface to boiling liquid

Re Reynolds number

T temperature

ΔT temperature difference, $T_w - T_{sat}$

t time

u velocity

u_o bubble rise velocity immediately following departure

x vertical distance from heated surface to bubble center of gravity

γ radius of curvature of bubble profile at its base

θ contact angle between bubble and heated surface

μ dynamic viscosity

ρ density

σ surface tension

Subscripts:

bu buoyancy

d drag

i inertial

l liquid

n normal (Earth) gravity

o at detachment

r rising through liquid

s surface tension

sat saturation

v vapor

w surface

ANALYSIS

Forces Acting on Bubbles During Growth

In this section the expressions to be used for computing the forces acting on a growing bubble are derived and briefly discussed. The bubbles obtained in the present experimental study were very nearly spherical as shown by the con-

tours reproduced in figure 4 (p. 15). Hence, a perfectly spherical bubble model was assumed in deriving expressions for the inertial and drag forces and for part of the buoyancy force.

Inertia. - The inertial force developed during the growth of a bubble is primarily the result of putting the surrounding fluid into motion. According to reference 10, the apparent mass of the affected fluid is that occupied by 11/16 of the bubble volume. The acceleration of the fluid is approximated as in references 5 and 6 by the time rate of change of the bubble growth velocity where the velocity is the change of radius with time. Then

$$F_i = \frac{d}{dt}(mu) = \frac{d}{dt}\left[\left(\frac{11}{16}\frac{\rho_l}{g_n}\frac{\pi D^3}{6}\right)\frac{1}{2}\frac{dD}{dt}\right]$$

which can be rewritten in the final form

$$F_i = \frac{11}{192}\frac{\pi\rho_l}{g_n}\left[D^3\frac{d^2D}{dt^2} + 3D^2\left(\frac{dD}{dt}\right)^2\right] \qquad (1)$$

Evaluating F_i analytically requires an expression for the bubble growth $D(t)$. Several analyses have yielded growth expressions of the form $D \sim t^n$, with the most simple expressions being of the type $D = ct^{1/2}$, where c is a constant that depends on the particular physical conditions. Experimentally, however, as in references 4 and 9, n ranges from approximately 1/2 to 1 during the early stages of growth and then decreases to approximately 1/3 in the later stages. The analysis of Forster (ref. 11) predicts a change in n from 1/2 to 1/4 during bubble growth and hence agrees qualitatively with the experimental behavior. The value of n is very important as a small difference in n can have a very large effect on F_i computed from equation (1). For example, if n is assumed to be constant with time and equal to 1/2, the inertial force is independent of time, while if $n = 3/8$, F_i varies as $t^{-1/2}$, and if $n = 1/4$, the inertial force becomes zero. Since experiments yield a range of bubble growth curves, characterizing the bubbles by a single type of inertial-force variation with time does not seem reasonable.

The approach in the present report is to evaluate the inertial force from measurements of specific bubbles so that comparisons can be made with the buoyancy and surface-tension forces obtained from the same bubbles. An accurate evaluation of equation (1) directly from bubble diameter measurements is impossible principally because the unavoidable scatter of the data points would produce large errors in the second derivative term d^2D/dt^2. Hence, the following procedure was utilized. A smooth curve for D as a function of t was drawn through the measurements taken from a single bubble. Then approximately 100 points were read from the curve and used in a least squares digital computer program to fit a sixth-order polynomial to the points. Sometimes it was necessary to fit a separate polynomial to each of two or three curves obtained by dividing the original curve into overlapping segments. After a polynomial had been obtained, results were evaluated from equation (1) by differentiating the polynomial analytically as required.

Buoyancy. - The buoyancy force is equal to the integral over the bubble surface of the vertical component of the hydrostatic pressure force. For an unattached spherical bubble this integration would yield simply

$$F = \frac{\pi D^3}{6} (\rho_l - \rho_v) \frac{g}{g_n}$$

When a bubble is attached to a surface, however, the buoyancy force must be modified to account for the pressures acting on the base area. The additional term that arises was considered in reference 12, where it was combined with the surface-tension force at the bubble base rather than more appropriately being included in the buoyancy force. The details of the evaluation are given in reference 13. With this additional term included, the buoyancy force for an attached bubble is given by

$$F_{bu} = \frac{\pi D^3}{6} (\rho_l - \rho_v) \frac{g}{g_n} + (p_b - P_b) \frac{\pi D_b^2}{4} \tag{2}$$

The pressure difference at the bubble base $p_b - P_b$ can be written in terms of the principal radii of curvature as

$$p_b - P_b = \frac{2\sigma \sin \theta}{D_b} + \frac{\sigma}{\gamma} \tag{3}$$

A difficulty in the evaluation of equation (3) is that accurate measurements of the radius of curvature γ of the bubble profile at the base are inherently difficult to obtain. The bubble profiles generally become less curved near the surface, however, particularly in the later stages of growth. Consequently, the radius of curvature at the bubble base is significantly larger than the bubble radius, making the second term on the right of equation (3) small compared with the first term. Hence, as an approximation, the σ/γ term will be neglected here. Then equation (2) becomes

$$F_{bu} = \frac{\pi D^3}{6} (\rho_l - \rho_v) \frac{g}{g_n} + \frac{\pi D_b}{2} \sigma \sin \theta \tag{4}$$

The second term on the right is equal to one-half the surface-tension force, as will be shown by equation (5). In reference 8, it is assumed that both of the principal radii of curvature are $D/2$. This assumption yields $p_b - P_b = 4\sigma/D$, which seems too large in view of the preceding discussion.

Surface tension. - The inertial and buoyancy forces are balanced by the surface-tension force, which holds the bubble base to the surface. The surface-tension force is given by

$$F_s = \pi D_b \sigma \sin \theta \tag{5}$$

Drag. - Only a very rough estimate of the drag force for a growing bubble could be made. A bubble growing on the surface was assumed to behave as a spherical vapor bubble rising through the liquid with a velocity equal to its change of radius with time. This assumption is only approximate since the top of a bubble has an upward velocity closer to dD/dt, while the remaining portions of the bubble have upward velocities ranging between dD/dt and zero. Also, a bubble freely rising through a liquid has a wake associated with it, and hence the use in the present case of a drag coefficient obtained from a freely rising bubble will tend to make the computed drag larger than that actually present. As discussed later, the drag coefficient used for a freely rising bubble has the form $C_d = a/Re$ where $a = 45$. The Reynolds number for the growing bubble is computed as a function of time from

$$Re = \frac{\rho_l D}{2\mu_l} \frac{dD}{dt}$$

The drag force is then obtained from

$$F_d = \frac{1}{2} \rho_l C_d \frac{\pi D^2}{4} \left(\frac{1}{2} \frac{dD}{dt}\right)^2 = \frac{\pi}{16} a\mu_l D \frac{dD}{dt} \tag{6}$$

Forces Acting on Bubbles After Departure

Following departure, a bubble accelerates away from the surface and eventually reaches a steady rise velocity. It is assumed that at any instant after departure the drag coefficient on a bubble accelerating away from the surface is the same as that for a bubble having a steady velocity equal to the instantaneous velocity of the accelerating bubble. The drag force is then $(\pi D_r^2/8)\rho_l u^2 C_d$. Using the apparent mass of the rising bubble, which is $(11/16)\rho_l(\pi D_r^3/6)$ as given in reference 10, gives the dynamic equation

$$\frac{1}{6} \pi D_r^3 g(\rho_l - \rho_v) - \frac{\pi D_r^2}{8} \rho_l u^2 C_d = \frac{11}{16} \rho_l \frac{\pi D_r^3}{6} \frac{du}{dt} \tag{7}$$

The drag coefficient depends on the bubble Reynolds number. For the present experiments, the maximum bubble velocity, which occurred for the normal gravity case, was about 10 inches per second (see fig. 6(b), p. 16) while the diameter of the bubbles at departure is a maximum of about 0.2 inch (see fig. 3, p. 15). Using the properties of 60-percent sucrose solution at about 220° F gives the Reynolds number $uD_r\rho_l/\mu \approx 500$. For Reynolds numbers in this range, the data in figure 3 of reference 14 show that the drag coefficient can be approximated by the relation $C_d = a/Re$, where a value of $a = 45$ is chosen here as passing reasonably well through the data. This choice agrees quite well with $a = 48$ obtained theoretically by Moore (ref. 15). The value $C_d = 45/Re$ was substituted into equation (7) and the resulting expression rearranged into the form

$$\frac{du}{dt} + \frac{12}{11}\frac{a\mu}{\rho_l D_r^2} u = \frac{16}{11} g \frac{\rho_l - \rho_v}{\rho_l} \tag{8}$$

This equation is integrated once to give the bubble velocity, and then, since $u = dx/dt$, it is integrated again to give the bubble height above the surface as a function of time:

$$x = x_o + \frac{u_o - A}{B}(1 - e^{-Bt}) + At \tag{9}$$

where

$$A = \frac{4}{3} g \frac{\rho_l - \rho_v}{a\mu} D_r^2$$

$$B = \frac{12}{11}\frac{a}{\rho_l}\frac{\mu}{D_r^2}$$

and u_o and x_o are, respectively, the bubble velocity and the height of the center of the bubble above the surface immediately following departure, with $t = 0$ being the time at the instant of departure. Equation (9) will be used later for comparisons with the data.

EXPERIMENTAL APPARATUS

The apparatus used to photograph single bubbles in reduced gravity fields from which bubble growth data were obtained for use in the preceding equations is described in this section. The apparatus is essentially the same as that of reference 4 and hence will be described only briefly.

Counterweighted Drop Tower

A simplified diagram of the drop tower used to obtain reduced gravity fields is shown in figure 1(a). The platform on which the test boiler is mounted descends 12.5 feet before being decelerated by a sand bed. Various gravity fields were obtained by using different counterweights to regulate the rate of descent. No attempt was made to overcome all the friction in the system and the resulting minimum gravity attainable was 0.014 g_n.

Test Boiler

The boiling test surface was at the upper end of a copper rod, which was heated at the base by two 500-watt cartridge heaters, as shown in figure 1(b). The circular boiling area was surrounded by a 0.030-inch-thick fin, which was an integral part of the rod. The entire piece was machined from a single large cylinder to prevent any boiling from cracks that might have developed between

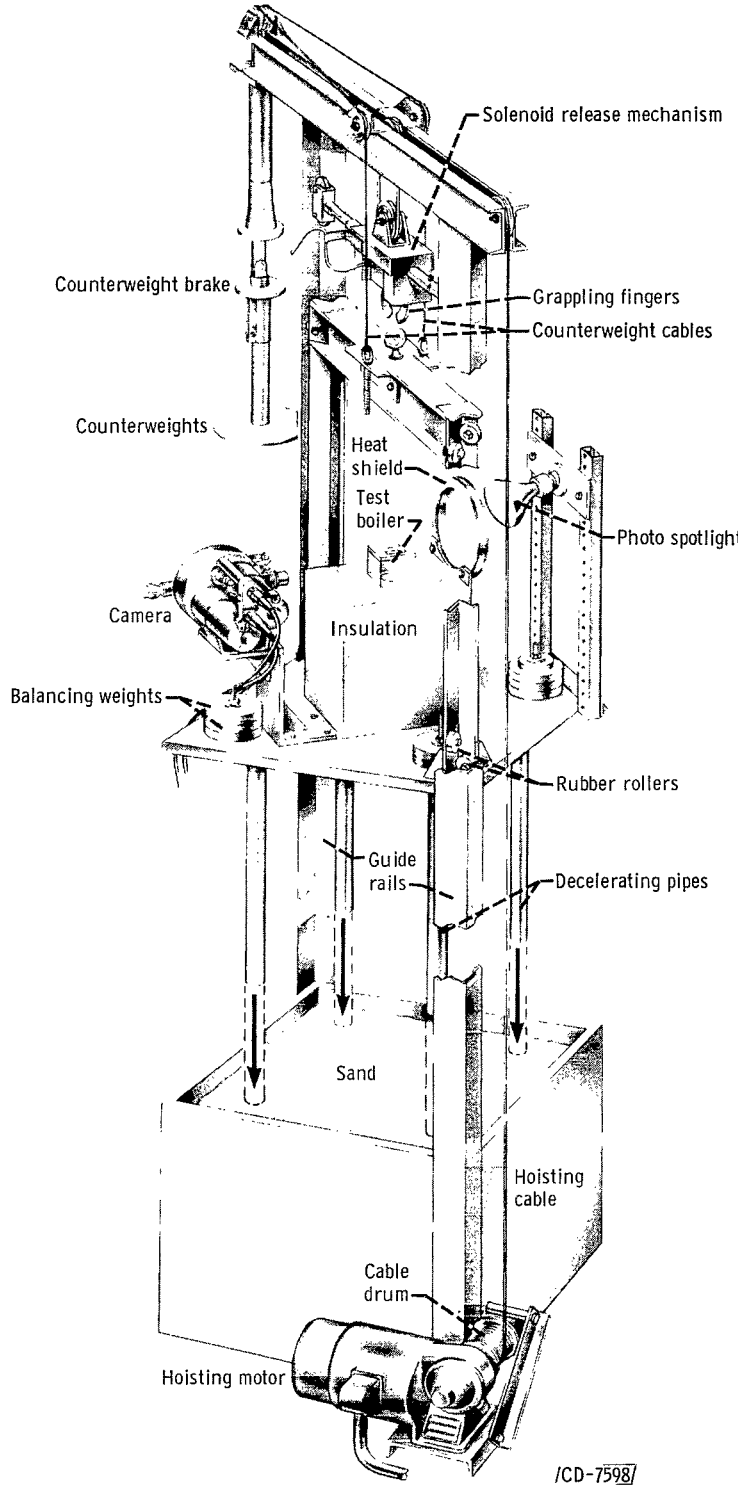

(a) Counterweighted drop tower. (Total height, 22.5 ft.).

Figure 1. - Experimental apparatus.

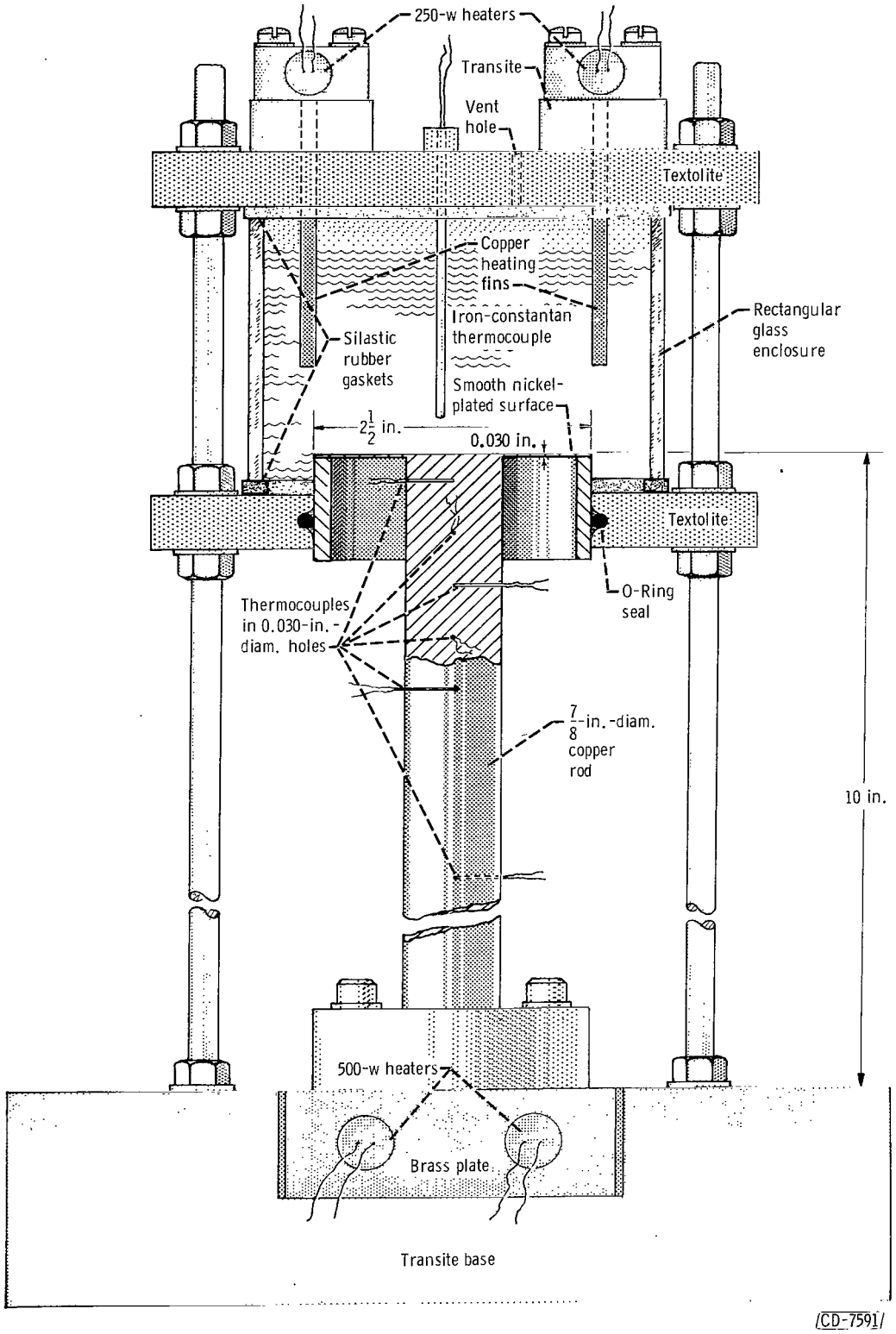

(b) Test boiler assembly.

Figure 1. - Concluded. Experimental apparatus.

the rod and the fin had they been two separate pieces. The fin attenuated the temperature so that boiling did not occur from the fin area or from the O-ring joint at the outside of the fin. Bubbles were thus prevented from rising in the foreground, which would have obscured photographs of the test area.

The present study attempts to deal with ideal bubbles originating from single nucleation sites spaced far enough apart that the bubble columns do not interfere with each other. The number of natural sites on the boiling surface was limited by polishing it with fine emery cloth and then lapping it to a 4-microinch root-mean-square roughness. It was then given a 0.0005-inch-thick nickel plating and polished with a paste of water and fine alumina. With this surface condition and a low heat flux, it was possible to obtain only a few nucleating bubble columns on the test area.

Two 250-watt cartridge heaters, mounted in copper fins extending through the top of the boiler, were used to maintain the liquid at the saturation temperature. The boiler was mounted in a box filled with powdered insulation so that only the test surface and glass enclosure were exposed.

Instrumentation

As shown in figure 1(b), iron-constantan thermocouples were mounted in 0.030-inch holes at several positions along the axial length of the copper rod. The temperature gradient along the rod permitted evaluation of the heat flux, and the surface temperature was obtained by extrapolating the temperature variation.

Photographs were taken with a 16-millimeter motion-picture camera with lens extension tubes to magnify the field. The camera speed was about 3500 frames per second, and a 500-cycle, square-wave generator was used to place timing marks on the film every 1/1000 of a second. Illumination was provided by a single 750-watt spotlight mounted about 5 inches above and 15 inches to the rear of the test surface, which gave good definition of the bubble outlines. A flat cell containing 1/2 inch of water between two pieces of plate glass was placed between the light and the boiler. The cell absorbed most of the heat from the light, and thus thermal equilibrium was not disturbed when the light was turned on.

The fluid temperature was measured with two thermocouples each mounted inside a stainless-steel tube 0.0625 inch in diameter. One of the tubes was extended into the photographic field to provide a standard size for calibrating the bubble measurements.

Experimental Procedure

The test surface was cleaned, polished, and wiped with tissue and distilled water, and the boiler was then assembled and filled with aqueous-sucrose solution. The upper heating fins were used to bring the solution to the saturation temperature and to drive off dissolved gases. The test section was heated slowly in order to activate only a few nucleation sites. The solution was

boiled for a few hours to achieve a steady-state condition and for deaeration. If the number of active sites was excessive, this procedure was repeated until a situation was obtained in which a steady stream of bubbles issued from only one or two sites.

The platform was raised into position and the counterweight loading adjusted to provide the desired gravity field. The photographic light was turned on, and a switch was then closed that simultaneously started the camera and a timer. After a preset time interval (usually about 1/4 sec), the timer activated a solenoid release, which dropped the platform. As soon as the platform started to move, it energized a microswitch in the pulse generator circuit, which placed a light flash on the film margin to identify the beginning of the reduced gravity period. Providing a time delay before the platform was released permitted nucleation under normal gravity conditions to be recorded on the first part of each film so that comparisons could be made with the reduced gravity period immediately following. The counterweight was then changed to provide another gravity field, and the runs were continued until the same nucleation site had been photographed in all the different gravity fields. Two or three 100-foot rolls of film were taken for each site at each gravity field. Thermocouple readings were taken only with the platform at rest, as the thermal capacity of the system was too large for significant temperature changes to occur during drops of approximately 1-second duration.

EXPERIMENTAL RESULTS

Distilled Water

Measurements of individual bubbles growing in saturated distilled water in reduced gravity are reported in reference 4. Some of these results will be briefly summarized here for comparison with the aqueous-sucrose data. The measurements were made on single bubbles growing from single nucleation sites without noticeable interference from adjacent bubbles. For this ideal type of bubble, it was found that as gravity was reduced, the bubble diameters at departure increased as $g^{-1/3}$ for fields between 0.1 and 1 g_n, and for lower gravities increased as $g^{-1/2}$. The latter functional relation is obtained theoretically by considering the bubble departure to be governed by a balance of only surface-tension and buoyancy forces. For the gravities closer to 1 g_n, the dynamic force appeared to be of some significance in changing the functional form of the gravity dependence from $g^{-1/2}$ to $g^{-1/3}$.

As gravity was reduced, the increase in bubble departure size was accompanied by much longer growth times. The growth curves of diameter as a function of time all had the same general shape with the curves for lower gravities just extending to larger diameters and times. If the bubble-diameter variation is expressed as $D \sim t^n$, n was found to range from 0.5 to 0.8 for $t < 0.02$ second and $n \approx 3/8$ for $t > 0.02$ second.

The contact angle remained essentially constant during growth. Also the contact angle did not change as gravity was reduced. The large bubbles in reduced gravity were accompanied by larger contact circle diameters at the bubble base.

Sucrose-Water Solutions

After the previous data for water had been obtained, it was desired to see if similar results would be found for fluids with different properties. Ethyl alcohol was tried, but single bubbles growing from a single site could not be obtained. As soon as a bubble would form, other smaller bubbles would be initiated around its base and merge with the original bubble. Also, at times the bubbles were observed to slide along the surface during growth.

In an effort to study the effect of fluid viscosity, an aqueous-sucrose solution was tried and this provided distinct single bubbles. Depending on the sucrose concentration, this fluid can be several times more viscous than water. The density is increased by only a small amount, however, and the surface tension remains close to that for water. The results for this fluid were considerably different from those for water. These differences will be explained later in terms of the forces acting on the bubbles.

Data were obtained for seven different gravity fields between 0.014 and 1.0 g_n for a 60-percent gravimetric sucrose solution. For 20- and 40-percent solutions, data were obtained in fields of 0.061, 0.229, and 1.0 g_n.

Reducing the gravity and increasing the viscosity substantially increased the merging of successive bubbles into a previously detached bubble. When the vapor mass formed by this merging had finally risen sufficiently far from the surface, the next bubble would grow undisturbed to its final departure size and then detach. Measurements were made only on the latter type of bubble.

Departure diameters. - Surprisingly, the departure diameters of the individual bubbles exhibited no definite gravity dependence. As mentioned previously, each roll of film recorded a period of normal gravity followed by the reduced gravity portion of the test. Table I gives some typical results for the departure diameters and growth times where each pair of entries was obtained from the data on a given roll of film. Each number represents an average for several bubbles. An arithmetic average was then taken for all the departure diameters in normal gravity in table I and gave an overall average normal-gravity bubble size of $D_{o,n} = 0.135$ inch. Each of the tabular values for reduced gravity was then divided by $D_{o,n}$ to give the data for site 1 in figure 2. This figure also shows data for another site in 60-percent sucrose solution and some data for several sites in 40- and 20-percent solutions. The heat fluxes and temperature differences for different test runs are given in

TABLE I. - AVERAGE DEPARTURE DIAMETERS AND GROWTH TIMES FOR BUBBLES IN 60-PERCENT GRAVIMETRIC AQUEOUS-SUCROSE SOLUTION AT NUCLEATION SITE 1

Percent of Earth gravitational field	Bubble diameter at detachment, D_o, in.	Growth time, sec	Percent of Earth gravitational field	Bubble diameter at detachment, D_o, in.	Growth time, sec
100	0.136	0.015	100	0.130	0.013
42.9	.152	.020	6.1	.140	.029
100	0.120	0.013	100	0.135	0.014
22.9	.150	.024	3.2	.137	.017
100	0.161	0.015	100	0.125	0.015
12.6	.142	.027	1.4	.201	.033

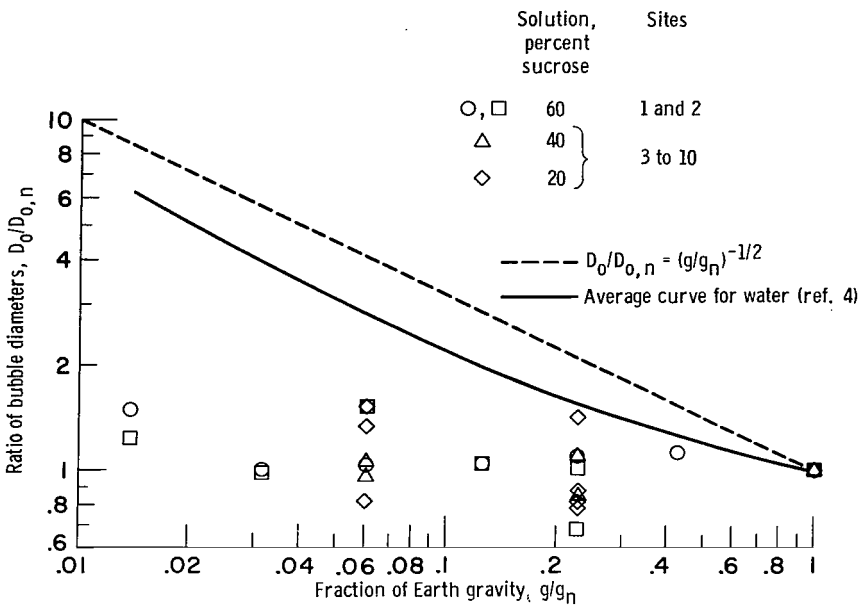

Figure 2. - Effect of reduced gravity on diameters of single undisturbed bubbles at instant of detachment from surface.

TABLE II. - HEAT FLUXES AND TEMPERATURE DIFFERENCES FOR DIFFERENT TEST RUNS

Site	Aqueous-sucrose solution, percent by weight	Heat transferred per unit area and time from solid surface to boiling liquid, q, Btu/(hr)(sq ft)	Temperature difference, $T_w - T_{sat}$, °F
1	60	20,500	30.1
2	60	18,800	29.8
3 to 6	40	21,900	21.4
7 to 10	20	21,500	19.5

Bubble growth. - Figure 3 is a logarithmic plot of some typical bubble-diameter variations with time for various gravity fields. The curves demonstrate the variations of growth behavior that can be encountered. These types of variations also occurred for bubbles in a single gravity field. Apparently no systematic variation of bubble growth with gravity occurred, although lowering the gravity field tended to produce longer growth times, as also illustrated in table I. The increase in growth time was small compared with that for water (ref. 4), where bubbles in low gravity had growth times an order of magnitude larger than in normal gravity. Even at the lowest gravities, the bubbles in 60-percent sucrose solution still had growth times as short as those for bubbles in water at normal gravity. The curve shapes in figure 3 demonstrate the difficulty in trying to characterize bubble growth by a simple relation of the form $D \sim t^n$ where the n exponent has a single value throughout the bubble lifetime.

Variation of contact angle and base width during growth. - The surface-tension force as given by equation (5) was evaluated from measurements made of the contact angle and the width of the bubble base from the bubble profiles throughout the bubble lifetime. If a thin microlayer of liquid were present beneath the bubble, such as has been postulated by some investigators, the actual dry surface area at the bubble base would be smaller than the measurements given here. The bubbles in sucrose were quite spherical (see profiles in fig. 4) and exhibited contact angles that were generally smaller than those in water. Because of the difficulty in measuring the slope of a curve, the absolute accuracy of the contact angles is approximately $\pm 10^{\circ}$.

For two typical bubbles, the contact angle and base widths during growth are shown in figure 5 for two different gravity fields. The contact angles ap-

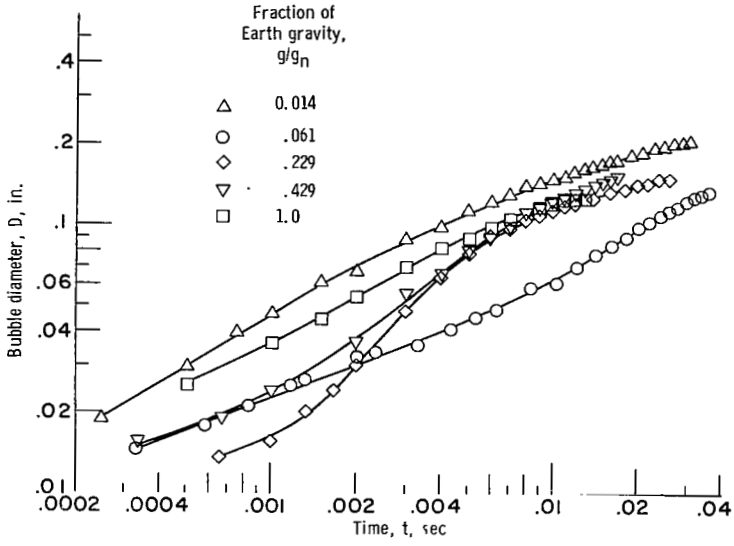

Figure 3. - Growth of typical undisturbed bubbles (at site 1 in 60-percent aqueous sucrose solution) for five gravity fields.

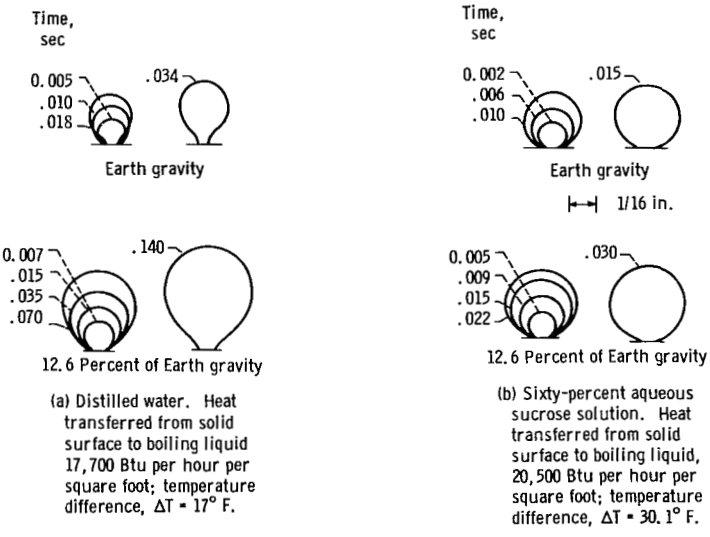

(a) Distilled water. Heat transferred from solid surface to boiling liquid 17,700 Btu per hour per square foot; temperature difference, $\Delta T = 17°$ F.

(b) Sixty-percent aqueous sucrose solution. Heat transferred from solid surface to boiling liquid, 20,500 Btu per hour per square foot; temperature difference, $\Delta T = 30.1°$ F.

Figure 4. - Profiles of bubbles during growth in normal and in reduced gravity.

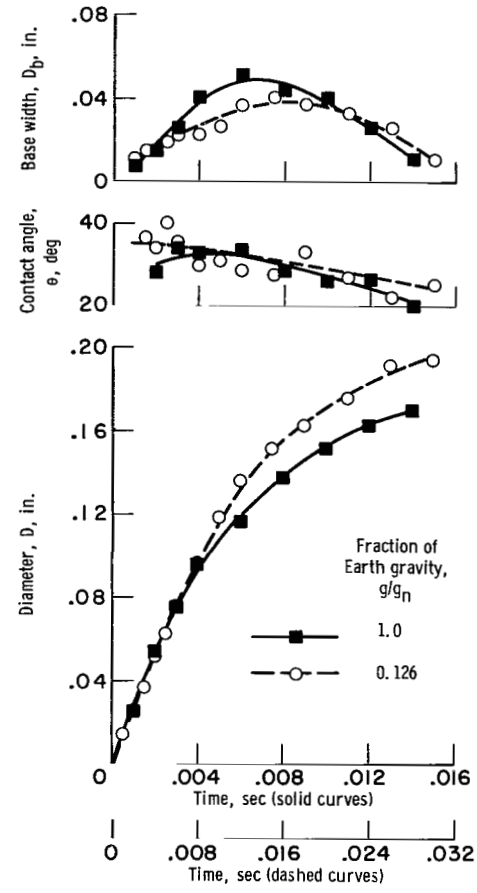

Figure 5. - Variation of diameter, contact angle, and base width with time for bubble growth in saturated 60-percent aqueous sucrose solution at site 1. Gravity fields, 1.0 and 0.126 g_n.

peared to decrease gradually with time during growth and were not dependent on the gravity field.

Behavior of bubbles after departure. - The motion of bubbles after departure is of interest when studying how the vapor is removed from the vicinity of the surface thereby preventing the formation of a vapor blanket. The velocity of a rising bubble will influence the coalescence of successive bubbles with it and perhaps the transition to continuous vapor columns (ref. 16). The motion of detached bubbles in reduced gravity fields is also of interest with regard to the collection of vapor in space-vehicle liquid-fuel tanks.

The data given here on bubble rise are for a 60-percent aqueous-sucrose solution. At site 1, bubbles formed in rapid succession with essentially zero waiting time between them; hence, successive bubbles often interfered or merged with each other. At site 2, however, the waiting times between bubbles were long - on the order of the bubble growth time. Hence, the bubbles rising from

site 2 were spaced sufficiently far apart that data could be obtained for individually rising bubbles. Figure 6(a) shows tracings of the profiles of a single bubble at site 2 for successive times after departure for each of three gravity fields. The distortion of the bubbles is reduced as gravity is decreased, and for 3.2-percent of normal gravity the bubble maintains its spherical shape. This indicates that the drag forces are small compared with the surface tension of the liquid-vapor interface that maintains the spherical shape. Although this behavior would be expected from the correlations of bubble shapes based on data in normal gravity, it has not been observed for the reduced gravity range. In figure 2 of reference 17, a collection of data is plotted that gives the ratio of horizontal to vertical diameter for freely rising bubbles as a function of the Eötvös number $E\ddot{o} = g(\rho_l - \rho_v)D_f^2/\sigma$, which is a ratio of buoyancy to surface-tension forces (re-

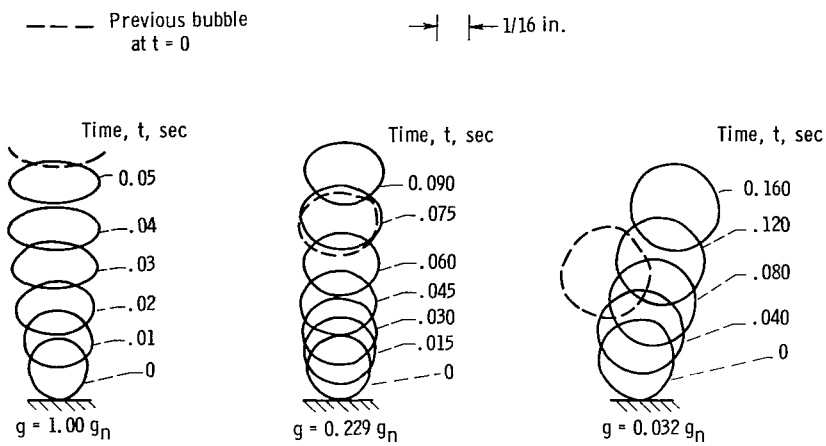

(a) Contours of rising bubbles.

Figure 6. - Motion of vapor bubbles after detachment at site 2 in 60-percent aqueous sucrose solution.

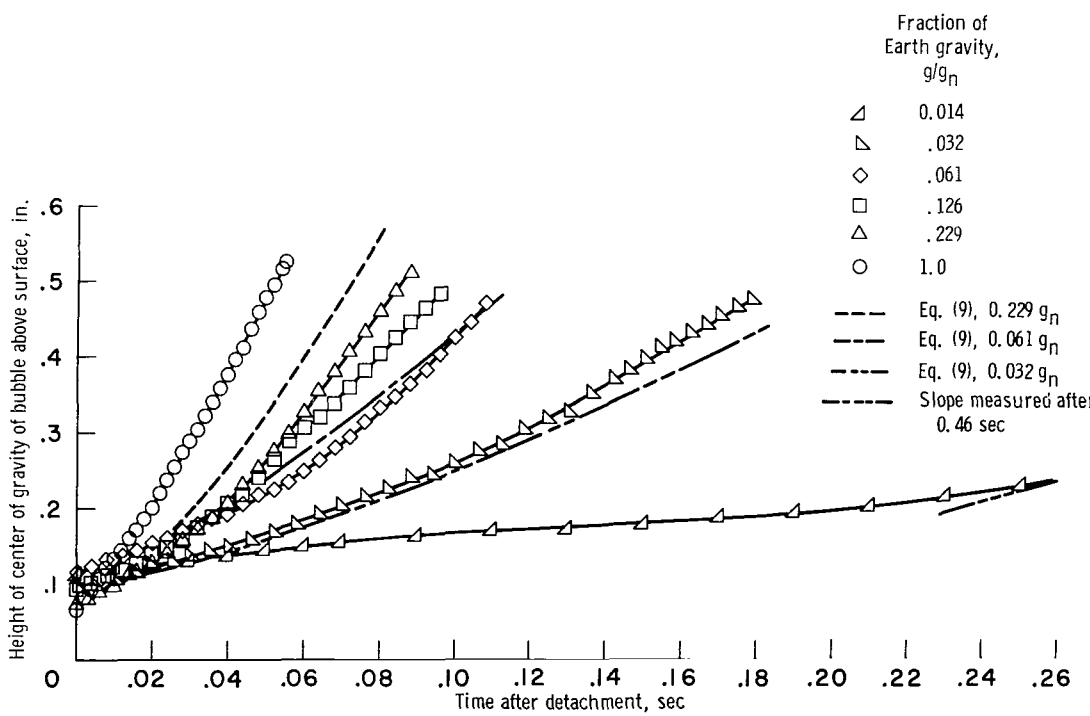

(b) Rise of center of gravity of bubbles for six gravity fields.

Figure 6. - Continued. Motion of vapor bubbles after detachment at site 2 in 60-percent aqueous sucrose solution.

ciprocal of the Bond number). At Eö ≈ 1, the ratio of diameters approaches unity. For the bubble at 0.032 g_n in figure 6(a), Eö ≈ 0.13, and, consequently, the surface tension is sufficiently large to maintain a spherical bubble shape. Hence, at low gravities the behavior of large bubbles that remain spherical, but which would become quite distorted in normal gravity, can be observed.

The rise of the center of gravity of typical bubbles after departure in six different gravity fields is shown in figure 6(b), and as expected, the rise velocity decreases with gravity. The rise immediately following bubble departure is given in detail in figure 6(c), which shows that the bubbles departed with a velocity larger than that immediately preceding detachment. Evidently, a propulsive force, possibly caused by fluid inertia, projects the bubbles from the surface. The upward velocity at detachment decreases as gravity is reduced, and at 3.2 percent g_n tends to become more nearly continuous with the velocity before departure.

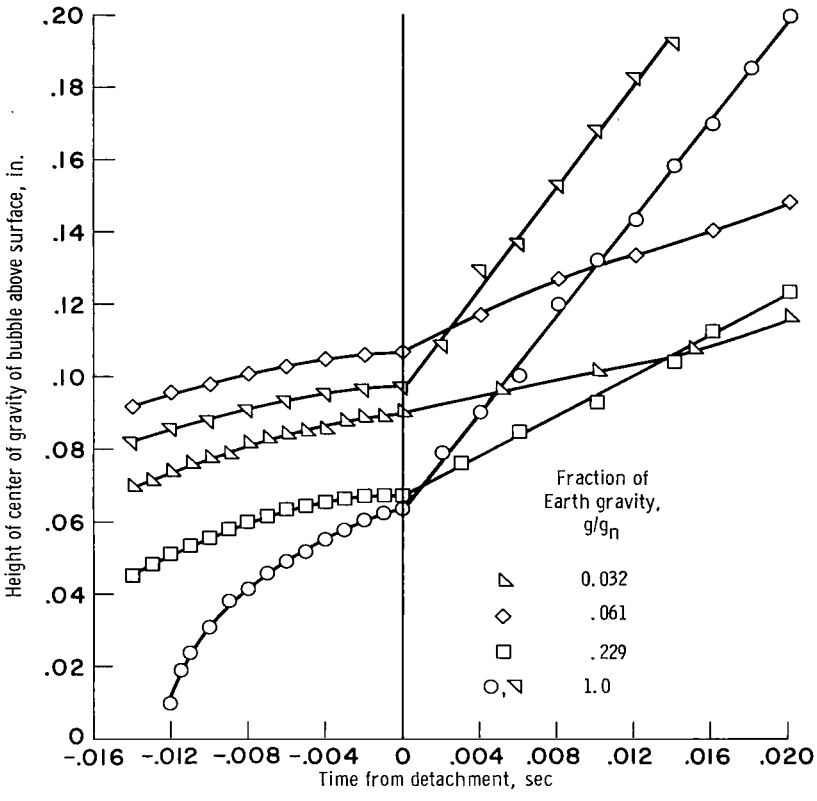

(c) Comparison of rise of center of gravity of vapor bubbles before and after detachment.

Figure 6. - Concluded. Motion of vapor bubbles after detachment at site 2 in 60-percent aqueous sucrose solution.

These experimentally obtained rise rates are compared with those predicted by equation (9), which was evaluated by using values of x_o and u_o obtained from figure 6(c). These experimental values are listed for three typical gravity fields in the table at the left. The theoretical curves in figure 6(b) seem to provide a reasonable prediction of the trends in the data. When the e^{-Bt} term in equation (9) becomes small, the steady rise velocity is achieved. In the present experiments, the times for which the bubbles could be observed before rising out of the field of view were insufficient for this velocity to be reached.

Fraction of Earth gravity, g/g_n	Distance from heated surface to bubble center of gravity at instant of bubble departure, x_o	Bubble rise velocity immediately following departure, u_o	Diameter of bubble while rising through liquid, D_r
0.032	0.090	1.15	0.180
.061	.107	2.10	.214
.229	.067	2.82	.148

DISCUSSION OF FORCES ACTING ON BUBBLES DURING GROWTH

As shown by figure 2 (p. 14), the data for bubble departure diameters in sucrose solutions tend to cluster about the constant line $D_o/D_{o,n} = 1$ so that gravity has no definite effect on the departure size over the range tested. This is in contrast with the results for water that exhibited a definite increase in bubble size as gravity was reduced. The independence of departure diameter as a function of gravity in sucrose solutions was somewhat unexpected, and the reasons for this behavior were not readily evident.

One factor thought to be of possible significance was the condition of the boiling surface. In both the tests with distilled water and with sucrose solutions, the same cleaning and polishing procedure was used. For some tests, boiling was initiated in pure distilled water and data taken, after which preheated high concentration sucrose solution was added to obtain the desired su-

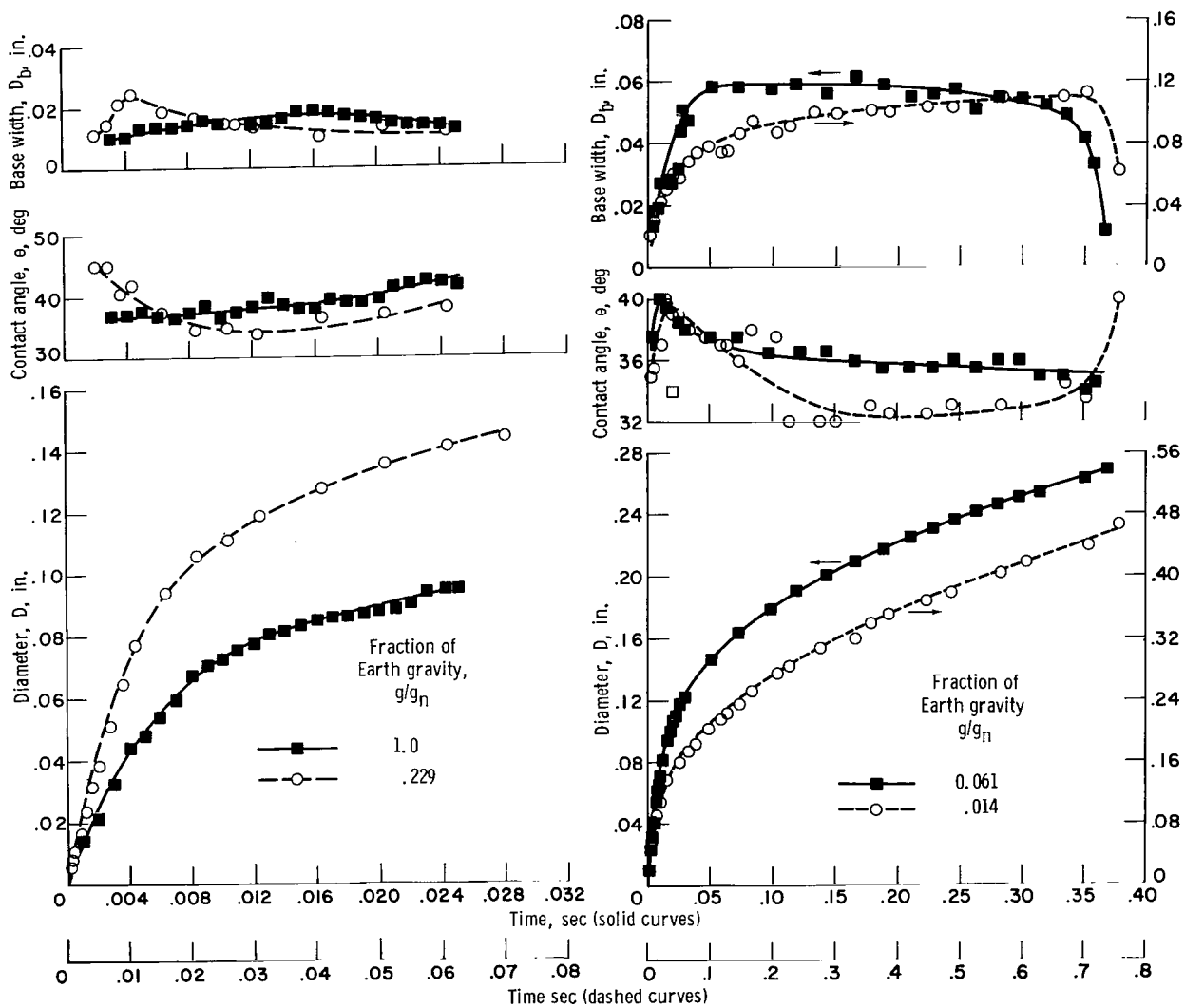

(a) Gravity fields, 1.0 and 0.229 g_n.

(b) Gravity fields, 0.061 and 0.014 g_n.

Figure 7. - Variation of diameter, contact angle, and base width with time for bubble growth in saturated water. Heat transferred from solid surface to boiling liquid, 10,900 Btu per hour per square foot; temperature difference, $\Delta T = 11.1°$ F.

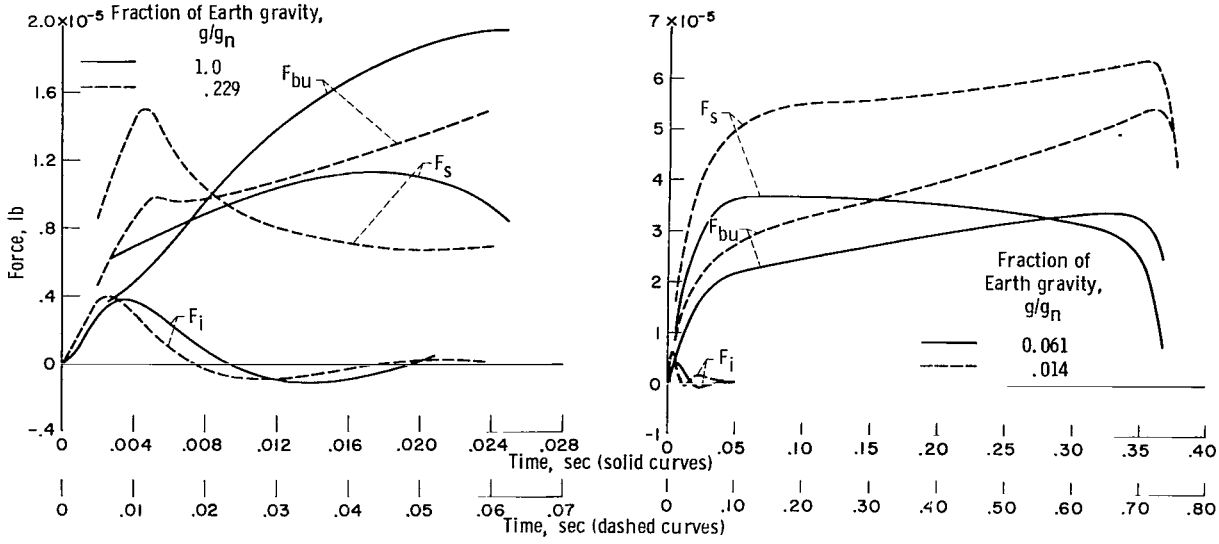

(a) Inertial, buoyancy, and surface-tension forces for bubbles in saturated water for 1.0 and 0.229 g_n gravity fields. Heat transferred from solid surface to boiling liquid, 10,900 Btu per hour per square foot; temperature difference, ΔT = 11.1° F.

(b) Inertial, buoyancy, and surface-tension forces for bubbles in saturated water for 0.061 and 0.014 g_n gravity fields. Heat transferred from solid surface to boiling liquid, 10,900 Btu per hour per square foot; temperature difference, ΔT = 11.1° F.

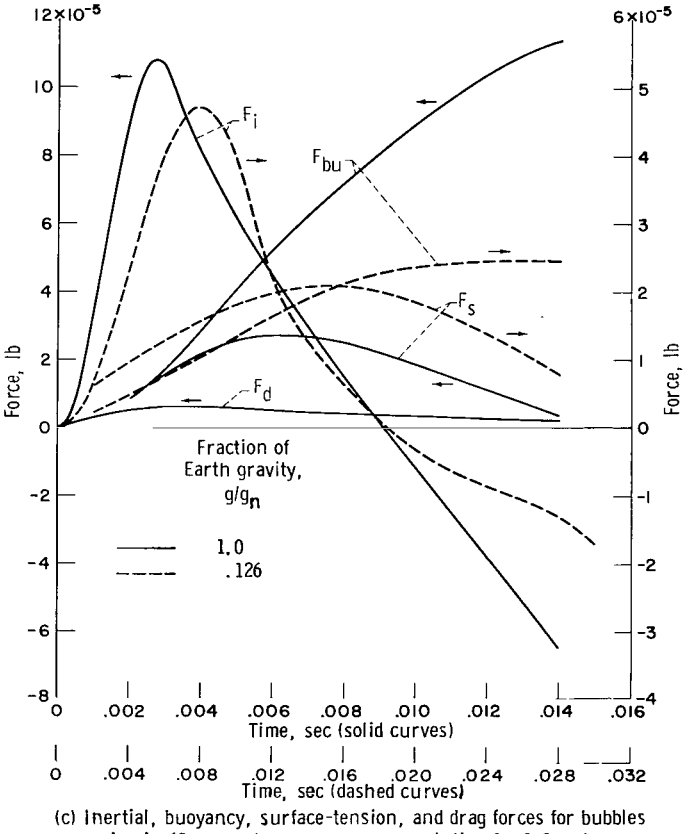

(c) Inertial, buoyancy, surface-tension, and drag forces for bubbles growing in 60-percent aqueous sucrose solution for 1.0 and 0.126 g_n gravity fields at site 1.

Figure 8. - Forces acting on growing bubbles.

crose concentration in the boiler. The same nucleation sites remained active throughout this procedure and, hence, the differences in boiling behavior in the two fluids cannot be attributed to simple mechanical variations of surface conditions.

To arrive at a possible explanation of the bubble departure behavior, an examination was made of the forces acting on a bubble during growth on the surface. In reference 4 measurements were made of bubble diameters, contact angles, and base diameters for saturated distilled water in several reduced gravity fields. Some of the data have been plotted in figure 7 for use in computing the forces acting on the bubbles. The buoyancy, surface-tension, and inertial forces have been computed throughout the growth period as described in the analysis and are shown in figure 8 for both boiling water and 60-percent aqueous-sucrose solu-

tion; the latter was computed from figure 5 (p. 15).

Figure 8(a) shows the forces for typical bubbles growing in water for Earth gravity and a reduced gravity field of 0.229 g_n. The magnitudes of the forces are quite similar for the two bubbles, and the only effect of the gravity reduction is an increase in the total growth time. Because of the rapid initial growth of either bubble, the inertial force reaches its maximum early in the growth period. By the time the inertial force reaches its maximum, however, the bubble base diameter has increased sufficiently to produce a surface-tension force that is somewhat larger than the inertial force. Hence, the maximum inertial force is insufficient to tear the bubble away from the surface. By pulling upward on the bubble, however, the inertia may impede the spreading of the bubble base and thus may have an influence in hastening bubble departure by retarding the buildup of the surface-tension force. The inertial force then decreases while the buoyancy force continues to increase. The buoyancy force eventually surpasses the surface-tension force so that the bubble must detach. Since a finite time is required for the bubble base to form a neck and finally break loose, the bubble continues to grow and, at departure, the buoyancy exceeds the surface-tension force.

Figure 8(b) shows the forces on bubbles in water for the much lower gravity fields 0.061 and 0.014 g_n. The total growth times are much longer than those of figure 8(a), and, consequently, the peak in the inertial force occurs early relative to the total growth period. As is shown in reference 4, the shape of the bubble growth curves for water were not very dependent on the gravitational field, which fixed only the time at which each growth curve terminated, and, hence, the maximum inertial forces in this low-gravity range have about the same magnitude as those in figure 8(a) for higher g's. As in figure 8(a), by the time the inertia has reached a maximum, the surface-tension force has become large enough to permit the bubble to continue to adhere to the surface. As growth continues, the inertia decreases and the bubble base continues to spread so that the surface-tension force becomes rather large. The buoyancy increases slowly because of the low-gravity field, but as the bubble becomes large, the buoyancy comes into balance with the surface-tension force and departure occurs. Hence, for the ideal type of bubbles photographed here, the departure in the very low-gravity range is dependent on the equilibrium of buoyancy and surface-tension forces. It is reasonable that the departure diameter in this range should depend on $g^{-1/2}$ since this variation is predicted by a balance of surface-tension and buoyancy forces, as in the Fritz equation. In reference 18, Semeria observed some bubbles in normal-gravity conditions that grew especially slowly after a short initial period of faster growth. These bubbles, which were termed Jakob bubbles, had departure diameters in agreement with the Fritz equation. This agreement is reasonable because for slowly growing bubbles, departure would be governed by buoyancy gradually overcoming the surface-tension force.

Figure 8(c) shows the forces computed for two typical bubbles growing in 60-percent aqueous-sucrose solution. The two sets of curves are similar to each other. One of the most important features of these curves is the large size of the inertial forces in comparison with the surface-tension forces. This is a result of the larger growth rates characteristic of the bubbles in sucrose as may be realized by comparing the growth curves in figures 5 and 7 (pp. 15 and

18, respectively). The larger growth rates may have been partly a result of the larger temperature differences existing for the sucrose solutions. As a result of the larger growth rates, the $(dD/dt)^2$ term in equation (1) contributes much more to the inertial force. For these bubbles, the large inertial force soon overcomes the surface-tension force and, hence, initiates bubble detachment. This detachment occurs when the buoyancy force is still small. Consequently, the departure process is dominated by inertia. As gravity is further reduced, the buoyancy becomes smaller and is even less important in influencing departure. Hence, the departure of the rapidly growing bubbles observed in sucrose solutions appears to be governed principally by inertia and surface-tension forces and does not exhibit a gravity dependence. Of course, the removal of the detached bubbles from the vicinity of the heated surface is still gravity dependent.

From the curves in figure 8, the following general observation can then be made. Apparently either inertia or buoyancy, or sometimes a combination of both, can initiate bubble departure. For the bubbles observed in distilled water, the inertial force may have had a small effect for gravity fields near normal gravity, but it became much smaller than the other forces in the lower gravity range (less than $0.126\ g_n$). Hence, departure was primarily the result of buoyancy overcoming the surface-tension force, and, therefore, the departure diameters exhibited a pronounced gravity dependence. For the bubbles observed in sucrose solutions, however, the growth rates were large and the resulting inertial forces were sufficiently high to cause bubble departure without the buoyancy force being significant. As a result, the departure in sucrose solutions was independent of gravity. It must not be inferred that all bubbles growing in water, for example, would be of the gravity-dependent type observed here. If a particular nucleation site emitted rapidly growing bubbles, these would most likely be gravity independent.

It is reported in the literature (ref. 19) that for subcooled boiling bubbles have sometimes been propelled away from the surface before condensing, even for a horizontal surface facing downward. Usually, however, the bubbles grow and collapse while remaining either attached or very close to the surface. The difference in behavior may result from the relative magnitudes of the inertial and surface-tension forces as discussed herein.

A force that has not been considered in the previous discussion is the viscous drag on a bubble during growth. As evidence of the influence of drag forces during bubble growth, Roll (ref. 20) observed in his experiments that the horizontal axis of a bubble growing on a surface was always greater than its vertical axis. It is stated that if the only force resisting upward motion were that due to surface tension, the vertical axis would be longer than the horizontal axis. In references 10 and 18, a flattening was noted in the first one-third to one-half of the growth period after which the vertical axis elongated.

For the present study of sucrose solutions, the behavior was somewhat surprising in that the bubbles were very nearly spherical during their entire growth period, as shown in figure 4, even though the growth times were more rapid than those for the water data, and the viscosity of the sucrose solution was several times greater than that for water. In an attempt to evaluate whether drag was significant, an approximate drag force was computed from equation (6). For

bubbles growing in water, the force ranged from 0.004×10^{-5} to 0.014×10^{-5} pound, the larger value occurring early in the growth period when the growth rate was large. For a 60-percent sucrose solution, the drag force increased to as high as 0.63×10^{-5} pound. A typical drag curve for the sucrose data is shown for the normal gravity case in figure 8(c). The values are generally small compared with the other forces shown in figure 8 and, hence, were not considered to influence bubble departure significantly.

CONCLUSIONS

Experimental measurements of single bubbles growing in aqueous-sucrose solutions were obtained in reduced gravity fields and used to compute the forces on the bubbles. The data from a previous experiment for boiling in distilled water were analyzed in a similar fashion, permitting the balance of forces for the different types of bubbles obtained in the two fluids to be compared. The following conclusions were made:

1. Bubble departure is governed by an interaction of buoyancy, inertial, and surface-tension forces with viscous drag playing only a minor role even for a highly viscous fluid such as 60-percent aqueous-sucrose solution.

2. For a rapidly growing bubble, the inertial force is sufficiently large to overcome the surface-tension force before buoyancy becomes significant. In this instance, the bubble departure does not depend on gravity, and the departure diameters are independent of a gravity reduction.

3. For a slowly growing bubble, the surface-tension force becomes large early in the growth period and exceeds the maximum inertial force before inertia can exert any effect. The inertia then decreases as the bubble growth continues, and buoyancy is the only force remaining to lift the bubble from the surface. In this case, since bubble departure is governed by a gravity-dependent force, the departure diameter is gravity dependent. Thus, depending on the bubble growth rate, bubble departure does or does not exhibit a gravity dependence.

4. After departure, the rise of a single bubble in 60-percent sucrose solution is predicted reasonably well for reduced gravity fields by using the drag coefficient $C_d = 45/Re$, where Re is the bubble Reynolds number.

5. The rapidly growing bubbles observed in 60-percent sucrose solution left the surface with a velocity higher than that given by the change of bubble radius with time immediately before departure. The velocities immediately before and after departure tended to become nearly equal as the gravity field was reduced.

Lewis Research Center
National Aeronautics and Space Administration
Cleveland, Ohio, April 30, 1964

REFERENCES

1. Usiskin, C. M., and Siegel, R.: An Experimental Study of Boiling in Reduced and Zero Gravity Fields. J. Heat Trans., ASME Trans., vol. 83, 1961, pp. 243-253.

2. Sherley, Joan E.: Nucleate Boiling Heat Transfer Data for Liquid Hydrogen at Standard and Zero-Gravity. Advances in Cryogenic Eng., vol. 8, K. D. Timmerhaus, ed., Plenum Press, 1963, pp. 495-500.

3. Merte, H., Jr., and Clark, J. A.: Boiling Heat Transfer with Cryogenic Fluids at Standard, Fractional, and Near-Zero Gravity. ASME Paper 63-HT-28, 1963.

4. Siegel, R., and Keshock, E. G.: Effects of Reduced Gravity on Nucleate Boiling Bubble Dynamics in Saturated Water. Preprint 3, AIChE 51st National Meeting, San Juan, Puerto Rico, Oct. 1963. (To be published in the AIChE Journal.)

5. Clark, J. A., and Merte, H., Jr.: Nucleate, Transition, and Film Boiling Heat Transfer at Zero Gravity. In: Advances in the Astro. Sci., vol. 14, Physical and Biological Phenomena in a Weightless State. American Astronautical Society, 1963, pp. 177-196.

6. Adelberg, M.: Gravitational Effect upon Nucleate Boiling Heat Transfer. In: Advances in the Astronautical Sciences, vol. 14. American Astronautical Society, 1963, pp. 196-223.

7. Forster, H. K., and Zuber, N.: Growth of a Vapor Bubble in a Superheated Liquid. J. Appl. Phys., vol. 25, 1954, pp. 474-478.

8. Chun, Ke-Sang: A Study of Steam Bubbles in Nucleate Boiling. Ph.D. Thesis, Ill. Inst. Tech., 1956.

9. Staniszewski, B. E.: Nucleate Boiling Bubble Growth and Departure. TR 16, Mass. Inst. Tech., Aug. 1959.

10. Han, C. Y., and Griffith, P.: The Mechanism of Heat Transfer in Nucleate Pool Boiling. TR 19, Mass. Inst. Tech., Feb. 1962.

11. Forster, K. E.: Growth of a Vapor-Filled Cavity Near a Heating Surface and Some Related Questions. Phys. Fluids, vol. 4, 1961, pp. 448-455.

12. Wark, Ian W.: The Physical Chemistry of Flotation. I - The Significance of Contact Angle in Flotation. J. Phys. Chem., vol. 37, 1933, pp. 623-644.

13. Sullivan, S. L., Jr., Hardy, B. W., and Holland, C. D.: Formation of Air Bubbles at Orifices Submerged Beneath Liquids. AIChE Paper 31E, Dec. 1963.

14. Gorring, Robert L., and Katz, Donald L.: Bubble Rise in a Packed Bed Saturated with Liquids. AIChE J., vol. 8, 1962, pp. 123-126.

15. Moore, D. W.: The Boundary Layer on a Spherical Gas Bubble. J. Fluid Mech., vol. 16, 1963, pp. 161-176.

16. Moissis, R., and Berenson, P. J.: On the Hydrodynamic Transitions in Nucleate Boiling. J. Heat Trans., ASME Trans., vol. 85, 1963, pp. 221-229.

17. Harmathy, Tibor Z.: Velocity of Large Drops and Bubbles in Media of Infinite or Restricted Extent. AIChE J., vol. 6, 1960, pp. 281-288.

18. Semeria, R. L.: An Experimental Study of the Characteristics of Vapour Bubbles. Paper 7, Symposium on Two Phase Fluid Flow, Institution of Mechanical Engineers, London, Feb. 1962, pp. 26-34.

19. Ibele, Warren E., ed.: Modern Developments in Heat Transfer. Heat Transfer with Boiling, W. M. Rohsenow, Academic Press, Inc., 1963, p. 111.

20. Roll, J. B.: The Effect of Surface Tension on Boiling Heat Transfer. Ph.D. Thesis, Purdue Univ., 1962.

NASA-Langley, 1964 E-2434

2-17-65

"The aeronautical and space activities of the United States shall be conducted so as to contribute . . . to the expansion of human knowledge of phenomena in the atmosphere and space. The Administration shall provide for the widest practicable and appropriate dissemination of information concerning its activities and the results thereof."

—NATIONAL AERONAUTICS AND SPACE ACT OF 1958

NASA SCIENTIFIC AND TECHNICAL PUBLICATIONS

TECHNICAL REPORTS: Scientific and technical information considered important, complete, and a lasting contribution to existing knowledge.

TECHNICAL NOTES: Information less broad in scope but nevertheless of importance as a contribution to existing knowledge.

TECHNICAL MEMORANDUMS: Information receiving limited distribution because of preliminary data, security classification, or other reasons.

CONTRACTOR REPORTS: Technical information generated in connection with a NASA contract or grant and released under NASA auspices.

TECHNICAL TRANSLATIONS: Information published in a foreign language considered to merit NASA distribution in English.

TECHNICAL REPRINTS: Information derived from NASA activities and initially published in the form of journal articles.

SPECIAL PUBLICATIONS: Information derived from or of value to NASA activities but not necessarily reporting the results of individual NASA-programmed scientific efforts. Publications include conference proceedings, monographs, data compilations, handbooks, sourcebooks, and special bibliographies.

Details on the availability of these publications may be obtained from:

SCIENTIFIC AND TECHNICAL INFORMATION DIVISION

NATIONAL AERONAUTICS AND SPACE ADMINISTRATION

Washington, D.C. 20546